

Understanding the stochastic dynamics of sequential decision-making processes: A path-integral analysis of Multi-armed Bandits

Bo Li^{1,2, a)} and Chi Ho Yeung^{3, b)}

¹⁾*School of Science, Harbin Institute of Technology (Shenzhen), Shenzhen, 518055, China*

²⁾*Non-linearity and Complexity Research Group, Aston University, Birmingham, B4 7ET, United Kingdom*

³⁾*Department of Science and Environmental Studies, The Education University of Hong Kong, 10 Lo Ping Road, Tai Po, Hong Kong*

The multi-armed bandit (MAB) model is one of the most classical models to study decision-making in an uncertain environment. In this model, a player needs to choose one of K possible arms of a bandit machine to play at each time step, where the corresponding arm returns a random reward to the player, potentially from a specific unknown distribution. The target of the player is to collect as much rewards as possible during the process. Despite its simplicity, the MAB model offers an excellent playground for studying the trade-off between exploration versus exploitation and designing effective algorithms for sequential decision-making under uncertainty. Although many asymptotically optimal algorithms have been established, the finite-time behaviours of the stochastic dynamics of the MAB model appears much more difficult to analyze, due to the intertwining between the decision-making and the rewards being collected. In this paper, we employ techniques in statistical physics to analyze the MAB model, which facilitates to characterize the distribution of cumulative regrets at a finite short time, the central quantity of interest in an MAB algorithm, as well as the intricate dynamical behaviours of the model.

Making decisions in an uncertain environment is a common and challenging task faced by human beings, other animals and intelligent machines. In such tasks, the decision-maker usually has several possible options, where the outcome of each option is unknown and stochastic. We investigate a scenario where the decision-maker has a limited budget to test the options, from which he/she gets rewards from the actions and simultaneously gains knowledge of the options with increasing confidence, which forms the basis of future decision-making among those repeated options. Such scenario constitutes a complex dynamical process where the decision-making and the collected rewards are intertwined, especially in finite time. To unveiled the nature of such complex dynamical processes, we apply methods from statistical physics to analyze the multi-armed bandit model, which is a prototypical mathematical model capturing the above characteristics of decision-making. The analytical distribution of the outcome of the decision-making process in finite time agrees well in simulations, and depict the origin of rare events where outcomes are much better or worse than expected can occur.

I. INTRODUCTION

Decision-making and optimization in uncertain environments are ubiquitous tasks faced by human beings, other natural creatures and intelligent machines. For example, animals have to decide on which unknown environment patches to search for food resources, which is crucial for their survival¹. Such tasks are also common in a pandemic situation, where one needs to decide on whether to adopt new life-saving medicines or vaccines with limited supporting evidence, or to research these medications to understand their pros and cons more thoroughly before decisions are made²; in terms of testing, to decide which areas or groups to prioritize testing resources without a comprehensive understanding of the infection mechanism when testing capacity is limited³. Sticking to familiar good solutions can fully exploit the knowledge from past experiences but may lose the opportunity to discover possible better solutions, which is sub-optimal in the long run. On the other extreme, always exploring new territories can increase the chance to search for the best solutions but the excessive exploration may incur a high cost. The root of such decision-making tasks is to strike a balance between exploration and exploitation⁴.

The multi-armed bandit problem is one of the most classical models to address this issue^{5,6}. In this model, the bandit machine consists of K independent arms; each arm $k \in \{1, 2, \dots, K\}$ will return a reward $x_k \in \mathbb{R}$ drawn from an unknown probability distribution $P_k(x_k)$ once it is pulled by the player. The task of the player is to choose an arm $a^t \in \{1, 2, \dots, K\}$ at time t based on the historical outcomes of the rewards $\{x_{a^\tau}^\tau\}_{\tau=0}^{t-1}$, in order to maximize the cumulative reward $R = \sum_{t=0}^T x_{a^t}^t$ for a time

^{a)}Electronic mail: libo2021@hit.edu.cn

^{b)}Electronic mail: chyeung@eduhk.hk

period T . We denote the expected reward of arm k as $\mu_k = \mathbb{E}_{P_k}[x_k]$, and define the best arm k^* as the arm having the largest expected reward $k^* = \arg \max_k \mu_k$. Maximizing the the cumulative rewards is equivalent to minimizing the cumulative regrets $r = \sum_{t=0}^T (\mu_* - x_{a^t}^t)$ with $\mu_* = \mu_{k^*}$ as the mean reward of the best arm, since μ_* is a constant. From the player's perspective, the regret is not accessible as μ_* is unknown, so the player will use the cumulative reward R as the objective function in practice. However, the cumulative regret r is more useful for theoretically assessing the player's strategy in hindsight.

Despite the simplicity of the MAB model, it captures the essential characteristics of decision-making under uncertainty, in that the rewards returned by each arm is probabilistic and that the player has to devise a strategy to make decisions based on the noisy observations. There exist a lot of research works on the multi-armed bandit models in the statistics and applied mathematics literature, most of which aim to bound the expected cumulative regrets in the long run. Notably, optimal asymptotic bounds are established for certain policies to play the bandit machines under some appropriate conditions of the reward distributions, which states that as the time period T increases, the expected regrets $\mathbb{E}[r]$ only grows as $O(\log T)$, provided that the gap is sufficiently large between the optimal and sub-optimal arms⁷. The MAB model and the corresponding optimal strategies also receive a lot of attentions in the fields of reinforcement learning and the optimization of black-box functions, since the theoretical understanding established on the former is relevant to the latter^{4,8}.

Most existing theoretical studies focus on the expected behaviours of MAB. However, even when a strategy is optimal in the average sense, it may still incur high regrets in some realizations of the processes due to fluctuations of the rewards or the actions of the player (if they are stochastic)^{9,10}. In some applications, safety is also of concern in addition to collecting more rewards on average, which may require a more conservative strategy in general. To this end, many risk-averse bandit algorithms were proposed^{11,12}. Most existing research efforts along this line addressed this issue by augmenting or replacing the expected rewards by some risk-aware measures (such as variance), and focused on devising algorithms for the new problems.

More in-depth understanding of the fine-grained probabilistic characteristics of the deviations from the average behaviors including rare events is important for such purposes, but it remains much less explored. Some developments in such directions were made recently by mapping some bandit algorithms onto stochastic differential equations and considering the asymptotic limit^{13,14}. From another perspective, the continual interactions between the player and the bandit machine constitute an interesting stochastic dynamical system, which may exhibit rich emergent behaviours.

In this study, we aim to investigate the probabilis-

tic nature of the regret distribution and shed light on the MAB model as a complex stochastic dynamical system through the lens of the large deviation analysis combined with a path-integral formalism from statistical physics^{15,16}, and to provide insights on decision-making processes under uncertainty. Comparing to many existing studies which are based on high-probability bounds and use the asymptotic limit of a long time (i.e. a large number of trials), our analysis can provide more detailed and explicit characteristics of MABs in less explored regimes more difficult to be analyzed, including those rare events with a small probability in a finite time. We emphasize that our target is not to introduce new bandit algorithm or improve existing methods.

II. THE MODEL

A. Problem formulation

The essential elements of the MAB model have been briefly introduced in Sec. I. Here we provide more details of the model and clarify the notations that will be used. We consider a fixed time period $0 \leq t \leq T$ of the game. At time $t = 0$, the player pulls each arm $k \in \{1, 2, \dots, K\}$ once to warm up the system, and receives the corresponding random reward $x_k^0 \sim P_k(x)$ for each arm k . This can be considered as a homogeneous initial exploration step. At each time step $t \in \{1, 2, \dots, T\}$, the player selects only one arm $a^t \in \{1, 2, \dots, K\}$ among all K options based on the historical observations of the model, and receives a random reward $x_{a^t}^t$ from the corresponding arm.

We denote n_k^t as the number of times that arm k has been pulled up to time t , and s_k^t as the total rewards received from arm k up to time t . The quantities n_k^t and s_k^t satisfy

$$n_k^0 = 1, \quad (1)$$

$$s_k^0 = x_k^0, \quad (2)$$

$$n_k^t = \sum_{\tau=1}^t \delta(a^\tau, k) + n_k^0, \quad (3)$$

$$s_k^t = \sum_{\tau=1}^t x_{a^\tau}^\tau \delta(a^\tau, k) + s_k^0, \quad (4)$$

where $\delta(\cdot, \cdot)$ is the Kronecker delta function. That is, the action a^τ at time τ has a contribution to n_k^t and s_k^t only if $a^\tau = k$ when $\tau \leq t$. We also adopt the shorthand notations of the vector along the time dimension $s_k^{0:T} := [s_k^0, s_k^1, \dots, s_k^T]$, and the vector along the arm dimension $\mathbf{s}^t := [s_1^t, s_2^t, \dots, s_K^t]$. Under these notations, the cumulative reward is $R = \sum_k s_k^T$ and the cumulative regret is $r = (T + K)\mu_* - \sum_k s_k^T$.

The policy (or algorithm) of a MAB model specifies a strategy of choosing an arm $k = a^{t+1}$ at time $t + 1$ based on previous actions $\{a^\tau\}_{\tau \leq t}$ and observations $\{x_{a^\tau}^\tau\}_{\tau \leq t}$. Due to the non-interacting nature of the basic MAB

model, it is convenient to consider the sum of historical choices and payoffs $\{n_{k'}^t, s_{k'}^t\}_{\forall k'}$ to determine which arm to pull at time t . In this case, the action a^{t+1} is a function of sum of these historical statistics as $a^{t+1}(\mathbf{n}^t, \mathbf{s}^t)$. Since the parameters of the distributions of the arms are unknown, we need to estimate them based on historical observations. For instance, after pulling the arm at time t , the expected reward of arm k can be estimated as

$$\hat{\mu}_k^t = \frac{s_k^t}{n_k^t}, \quad (5)$$

which will be used by the player for determining which arm to pull in the future.

B. Bandit Algorithms

A simple strategy for optimizing outcomes from the MAB model is to perform the following two-stage operation (i) allocate a fixed number of trials to each arm k to estimate the expected reward $\hat{\mu}_k$ by Eq. (5) (this is a purely exploration phase); (ii) identify the estimated best arm $\hat{k}^* = \arg \max_k \hat{\mu}_k$ and keep pulling it in the future steps (this is a purely exploitation phase). In order to precisely estimate the arm parameters for the benefit of the second stage, a substantial amount of resources is needed to explore all arms, resulting in low rewards being collected from the non-optimal arms in the first stage. On the other hand, if less resources are spent in the first stage for exploration, then the player has a higher risk of incorrectly identifying the best arm. Many real life problems are solved by this policy, e.g., in clinical trials, it is usual to perform a predefined amount of experimental trials to choose one medicine or vaccine among several possible options and then deploy the chosen one widely. Such a policy can be sub-optimal for the purpose of maximizing the cumulative rewards. Many research efforts are devoted to finding a better policy (or algorithm) for MAB which strikes a balance between exploration and exploitation.

1. ϵ -greedy Algorithm

An alternative strategy is to perform exploration and exploitation stochastically in an online fashion. In the ϵ -greedy algorithm⁴, at each time step, the player either chooses the estimated best arm to pull (with probability $1 - \epsilon$), or selects a random arm to explore (with probability ϵ). The probability ϵ controls the amount of exploration, which can vary over time.

2. Softmax Algorithm

Another stochastic algorithm is the softmax method⁴, which picks an arm at time $t + 1$ according to a Boltz-

mann distribution

$$p_k^{t+1} = \frac{e^{\beta \hat{\mu}_k^t}}{\sum_{j=1}^K e^{\beta \hat{\mu}_j^t}}, \quad (6)$$

where β is the inverse temperature parameter controlling the amount of exploration. For a small β , it tends to explore more uniformly among different arms, while for a large β , it tends to exploit the estimated best arm. The inverse temperature can also vary over time.

C. UCB Algorithm

Despite the simplicity of the above-mentioned stochastic algorithms, they either yield sub-optimal total rewards or require carefully tuning the parameters. Another important class of bandit algorithms, the upper confidence bounds (UCB) algorithms, stem from more solid theoretical properties and achieve optimal asymptotic total rewards on average^{5,6,17}. It starts by computing the upper confidence bound (UCB) of the sample mean estimation for each arm k as

$$B_k^t = \frac{s_k^t}{n_k^t} + b^t \frac{1}{\sqrt{n_k^t}}, \quad (7)$$

where the parameter b^t controls the confidence level, which can vary over time. Since the sample standard deviation of a certain random variable is proportional to $1/\sqrt{n}$ after n independent measurements, Eq. (7) represents an upper confidence bound for reward x_k after n_k^t measurements on arm k . The UCB algorithm proceeds by selecting the arm corresponding to highest UCB index $a^{t+1} = \arg \max_k B_k^t$, which is a principle of ‘‘optimism in the face of uncertainty’’ (by comparing the best possibilities of all arms in a certain confidence level).

The two terms of the UCB index in Eq. (7) represent the effects of exploitation and exploration, respectively. The second term of Eq. (7) encourages exploration because if an arm k has a low n_k^t (low exploration of the arm up to time t), then the second term is large for arm k , which increases its UCB index and the chance that arm k is being pulled.

If the rewards have bounded range, e.g., $0 \leq x_k \leq 1$, it is sufficient to achieve the optimal asymptotic regret bound of $O(\log(T))$ by setting the tuning parameter b^{t-1} in Eq. (7) as $b^t = c\sqrt{\log(K+t)}$, where c is a parameter tuning the level of exploration; notice that $K+t$ is the total number of arm pulls until time t .

D. MABs as Stochastic Dynamical Systems

Despite the simplicity of the problem formulation, the MABs represent fairly complex decision-making process from the dynamical system perspective, as the random rewards being collected will impact on the decisions in

future rounds, and this will in turn impact on the estimate of rewards given by individual arms and hence the reward given by the bandit machine in the future.

To disentangle such complex dynamics, we will adopt methods from statistical physics on stochastic dynamical systems for analyzing MABs. To this end, we consider the probabilistic evolution of the action $\{a^t\}_{1 \leq t \leq T}$ in the form of, given by

$$B_k^t(s_k^t, n_k^t) = \frac{s_k^t}{n_k^t} + c \sqrt{\frac{\log(K+t)}{n_k^t}}, \quad (8)$$

$$P(a^{t+1} = k) = \frac{e^{\beta B_k^t(s_k^t, n_k^t)}}{\sum_j e^{\beta B_j^t(s_j^t, n_j^t)}}, \quad t \geq 0, \quad (9)$$

which is a combination of the softmax and UCB strategies. In the infinite β (zero temperature) limit, Eq. (9) reduces to the UCB algorithm. On the other hand, it becomes the traditional softmax algorithm when $c = 0$.

In this work, we specify the arm reward distributions as Gaussian distributions,

$$P(x_k^t) = \mathcal{N}(x_k^t | \mu_k, \sigma_k^2). \quad (10)$$

III. STATISTICAL-PHYSICS ANALYSIS

We now proceed to analyze the stochastic dynamical process of MABs by adopting methods from statistical physics. The quantity of interest is the probability distribution of the cumulative regret

$$\begin{aligned} P(r) &= \left\langle \delta \left[r - ((T+K)\mu_* - \sum_k s_k^T) \right] \right\rangle_{a^{1:T}, \mathbf{x}^{0:T}}, \\ &= \int \prod_{t=0}^{T-1} d\mathbf{x}^t P(\mathbf{x}^t) \prod_{t=1}^T \sum_{a^t} P(a^t) \\ &\quad \times \delta \left(r + \sum_k s_k^T - (T+K)\mu_* \right), \end{aligned} \quad (11)$$

where the average is taken over the dynamical variables $a^{1:T}$ and $\mathbf{x}^{0:T}$ with respect to the distributions given in Eq. (9) and Eq. (10).

A. Path-integral Formalism

We note that in Eq. (9), the variables s_k^t and n_k^t also depend on the historical trajectories $a^{1:t}$ and $\mathbf{x}^{0:t}$ through Eq. (3) and Eq. (4), making the average in Eq. (11) highly non-trivial. Borrowing methods from statistical physics, we consider $\{r, \mathbf{n}^{0:T}, \mathbf{s}^{0:T}\}$ as statistical fields and adopt the path-integral formalism for computing this average.

We first express the delta function in Eq. (11) by its Fourier representation

$$\delta \left(r + \sum_k s_k^T - (T+K)\mu_* \right) = \int \frac{d\hat{r}}{2\pi} e^{-i\hat{r} \left(r + \sum_k s_k^T - (T+K)\mu_* \right)}, \quad (12)$$

and insert the Fourier representation of unities for $\{s_k^t, n_k^t\}$ through the definition in Eq. (1)-Eq. (4) to Eq. (11)

$$1 = \int \frac{d\hat{n}_k^0 dn_k^0}{2\pi} \exp \left[-i\hat{n}_k^0 (n_k^0 - 1) \right], \quad (13)$$

$$1 = \int \frac{d\hat{s}_k^0 ds_k^0}{2\pi} \exp \left[-i\hat{s}_k^0 (s_k^0 - x_k^0) \right], \quad (14)$$

$$1 = \int \frac{d\hat{n}_k^t dn_k^t}{2\pi} \exp \left[-i\hat{n}_k^t \left(n_k^t - 1 - \sum_{\tau=1}^t \delta(a^\tau, k) \right) \right], \quad (15)$$

$$1 = \int \frac{d\hat{s}_k^t ds_k^t}{2\pi} \exp \left[-i\hat{s}_k^t \left(s_k^t - x_k^0 - \sum_{\tau=1}^t x_k^\tau \delta(a^\tau, k) \right) \right], \quad (16)$$

after which Eq. (11) becomes

$$\begin{aligned} P(r) &= \int \prod_{t=0}^T d\mathbf{x}^t P(\mathbf{x}^t) \int \prod_{k=1}^K \prod_{t=0}^T \frac{d\hat{s}_k^t ds_k^t}{2\pi} \frac{d\hat{n}_k^t dn_k^t}{2\pi} \frac{d\hat{r}}{2\pi} \\ &\quad \sum_{\{a^t\}_{t=1}^T} \prod_{t=1}^T \left[e^{\beta B_{a^t}^{t-1}(s_{a^t}^{t-1}, n_{a^t}^{t-1})} / \sum_{k'=1}^K e^{\beta B_{k'}^{t-1}(s_{k'}^{t-1}, n_{k'}^{t-1})} \right] \\ &\quad \times \exp \left\{ -i\hat{r} \left(r + \sum_k s_k^T - (T+K)\mu_* \right) \right\} \\ &\quad \times \exp \left\{ -i \sum_{k=1}^K \left[\hat{s}_k^0 (s_k^0 - x_k^0) + \hat{n}_k^0 (n_k^0 - 1) \right] \right\} \\ &\quad \times \exp \left\{ -i \sum_{k=1}^K \sum_{t=1}^T \hat{s}_k^t \left(s_k^t - x_k^0 - \sum_{\tau=1}^t x_k^\tau \delta(a^\tau, k) \right) \right\} \\ &\quad \times \exp \left\{ -i \sum_{k=1}^K \sum_{t=1}^T \hat{n}_k^t \left(n_k^t - 1 - \sum_{\tau=1}^t \delta(a^\tau, k) \right) \right\}. \end{aligned} \quad (17)$$

In the second line of Eq. (17), the variables $\{s_k^t, n_k^t\}$ are stochastic fields which do not explicitly depend on $a^{1:t}$ and $\mathbf{x}^{0:t}$. Instead, such dependencies are expressed through their coupling to the conjugate fields $\{\hat{s}_k^t, \hat{n}_k^t\}$.

Now the average over the disorder variables $\mathbf{x}^{0:T}$ in Eq. (17) can be easily perform by using the identity $\int e^{-ixh} \mathcal{N}(x|\mu, \sigma^2) dx = e^{-\frac{1}{2}\sigma^2 h^2 - i\mu h}$, such that the distribution of regret $P(r)$ has the form of

$$P(r) = \int \prod_{k=1}^K \prod_{t=0}^T \frac{d\hat{s}_k^t ds_k^t}{2\pi} \frac{d\hat{n}_k^t dn_k^t}{2\pi} \frac{d\hat{r}}{2\pi} e^{-\Phi}, \quad (18)$$

where Φ is a stochastic action defined as

$$\begin{aligned} \Phi = & \text{i}\hat{r} \left(r + \sum_k s_k^T - (T + K)\mu_* \right) \\ & + \text{i} \sum_k \sum_{t=0}^T (\hat{s}_k^t s_k^t + \hat{n}_k^t (n_k^t - 1)) \\ & + \frac{1}{2} \sum_k \sigma_k^2 \sum_{t,t'=0}^T \hat{s}_k^t \hat{s}_k^{t'} n_k^{\min(t,t')} - \text{i} \sum_k \mu_k \sum_{t=0}^T \hat{s}_k^t n_k^t \\ & - \sum_{t=1}^T \left\{ \log \sum_k \exp \left[\beta B_k^{t-1}(s_k^{t-1}, n_k^{t-1}) + \text{i} \sum_{\tau=t}^T \hat{n}_k^\tau \right] \right. \\ & \left. - \log \sum_k e^{\beta B_k^{t-1}(s_k^{t-1}, n_k^{t-1})} \right\}. \end{aligned} \quad (19)$$

See Appendix A for details of the calculations. The action function Φ is reminiscent of a thermodynamic potential, which expresses the stochastic dynamical system through the order parameters $\{s_k^t, n_k^t, \hat{s}_k^t, \hat{n}_k^t\}$ of all time steps. Hence, Eq. (18) is a discrete-time path integral.

B. Small Noise Limit and Saddle-point Equations

An exact expression of Eq. (18) is difficult to obtain. To facilitate further analysis, we focus on the limit of low temperature and small arm noise $\beta \rightarrow \infty, \sigma_k \rightarrow 0$, which essentially consider the large deviation of the regret under the UCB algorithm¹⁸. This is because when the noise is small, the regret r has a high probability to be near its most probable value r^{mpv} ; in this case a sufficiently strong departure of r from r^{mpv} become rare events, which is the focus of large deviation theory in terms of probability^{15,18}. Although the theory is built on such a small noise limit, we expect some physical properties of the system still hold in the finite noise case, which is another interesting regime of the MAB problem.

In the small noise limit, for a particular value of regret r , the path integral in Eq. (18) is dictated by the saddle point of the action function Φ ¹⁸, which satisfies $\partial\Phi/\partial y = 0, y \in \{s_k^t, n_k^t, \hat{s}_k^t, \hat{n}_k^t, \hat{r}\}$.

To make the notations more compact, we define the following quantities

$$B_k^t = B_k^t(s_k^t, n_k^t), \quad (20)$$

$$B_{s,k}^t = \frac{\partial B_k^t(s_k^t, n_k^t)}{\partial s_k^t}, \quad (21)$$

$$B_{n,k}^t = \frac{\partial B_k^t(s_k^t, n_k^t)}{\partial n_k^t}, \quad (22)$$

$$\rho_k(\mathbf{v}) = \frac{e^{v_k}}{\sum_{j=1}^K e^{v_j}}, \quad (23)$$

$$h_k^{t+1} = \beta B_k^t(s_k^t, n_k^t) + \text{i} \sum_{\tau>t}^T \hat{n}_k^\tau, \quad (24)$$

where $\rho_k(\cdot)$ is the softmax operator.

Then the saddle point equations admit the following expressions

$$n_k^0 = 1, \quad (25)$$

$$n_k^t = 1 + \sum_{\tau=1}^t \rho_k(\mathbf{h}^\tau), \quad 1 \leq t \leq T, \quad (26)$$

$$s_k^t = \mu_k n_k^t + \sigma_k^2 \sum_{t'=0}^T (\text{i}\hat{s}_k^{t'}) n_k^{\min(t,t')}, \quad 0 \leq t \leq T, \quad (27)$$

$$\text{i}\hat{s}_k^t = \beta B_{s,k}^t [\rho_k(\mathbf{h}^{t+1}) - \rho_k(\beta \mathbf{B}^t)], \quad 0 \leq t < T, \quad (28)$$

$$\text{i}\hat{s}_k^T = -\text{i}\hat{r}, \quad (29)$$

$$\begin{aligned} \text{i}\hat{n}_k^t = & \beta B_{n,k}^t [\rho_k(\mathbf{h}^{t+1}) - \rho_k(\beta \mathbf{B}^t)] + \mu_k \text{i}\hat{s}_k^t \\ & - \sigma_k^2 \sum_{t'>t}^T \hat{s}_k^t \hat{s}_k^{t'} - \frac{1}{2} \sigma_k^2 (\hat{s}_k^t)^2, \quad 0 \leq t < T, \end{aligned} \quad (30)$$

$$\text{i}\hat{n}_k^T = \mu_k \text{i}\hat{s}_k^T - \frac{1}{2} \sigma_k^2 (\hat{s}_k^T)^2, \quad (31)$$

$$r = (T + K)\mu_* - \sum_k s_k^T, \quad (32)$$

where the last equation is a constraint for the total reward $\sum_k s_k^T$ (we remind that r is a pre-defined parameter instead of a dynamical variable). We remark that the conjugate fields $\{\hat{s}_k^t, \hat{n}_k^t, \hat{r}\}$ are defined on the imaginary axis in the saddle point^{19,20}.

C. Simplification in the Large β Limit

Further simplification can be made by exploiting the limit $\beta \rightarrow \infty$ under consideration. In this limit, the field h_k^{t+1} is dominated by βB_k^t , so that Eq. (26) can be approximated as

$$n_k^t = 1 + \sum_{\tau=1}^t \rho_k(\beta \mathbf{B}^{\tau-1}), \quad 1 \leq t \leq T, \quad (33)$$

To derive the dynamics of the conjugate order parameters $\{\hat{s}_k^t, \hat{n}_k^t\}_{t<T}$ in this limit, we notice

$$\begin{aligned} \rho_k(\mathbf{h}^{t+1}) & \approx \rho_k(\beta \mathbf{B}^t) + \sum_{j=1}^K \frac{\partial \rho_k(\mathbf{h}^{t+1})}{\partial h_j^{t+1}} \Big|_{\mathbf{h}^{t+1}=\beta \mathbf{B}^t} \cdot \text{i} \sum_{\tau>t}^T \hat{n}_j^\tau \\ & =: \rho_k(\beta \mathbf{B}^t) + \hat{\Delta} \rho^{t+1}(\beta \mathbf{B}^t) \cdot \sum_{\tau>t}^T \text{i} \mathbf{n}^\tau, \end{aligned} \quad (34)$$

where the $K \times K$ matrix $\hat{\Delta} \rho^{t+1}(\beta \mathbf{B}^t)$ has the element $\hat{\Delta} \rho^{t+1}(\beta \mathbf{B}^t)_{kj} = \delta_{jk} \rho_k(\beta \mathbf{B}^t) - \rho_k(\beta \mathbf{B}^t) \rho_j(\beta \mathbf{B}^t)$.

Under this approximation, the dynamical rules of

Eq. (28) and Eq. (30) become

$$i\hat{s}_k^t = \beta B_{s,k}^t \sum_j \hat{\Delta}\rho_{kj}^{t+1} \sum_{\tau>t} i\hat{n}_j^\tau, \quad (35)$$

$$i\hat{n}_k^t = \beta B_{n,k}^t \sum_j \hat{\Delta}\rho_{kj}^{t+1} \sum_{\tau>t} i\hat{n}_j^\tau + \mu_k i\hat{s}_k^t + \sigma_k^2 \sum_{t'>t} (i\hat{s}_k^t)(i\hat{s}_k^{t'}) + \frac{1}{2}\sigma_k^2 (i\hat{s}_k^t)^2, \quad (36)$$

which admit a backward iteration form.

In such a large β limit, the stochastic action Φ *evaluated at the saddle point* has a simple expression

$$\Phi^*(r|\sigma_k) = \frac{1}{2} \sum_k \sigma_k^2 \sum_{t,t'=0}^T (i\hat{s}_k^t)(i\hat{s}_k^{t'}) n_k^{\min(t,t')}. \quad (37)$$

We notice that if the variances of all arms are rescaled by a common factor γ , i.e., $\sigma_k^2 \rightarrow \gamma\sigma_k^2$, then the conjugate order parameters $\{\hat{s}_k^t, \hat{n}_k^t, \hat{r}\}$ evaluated at the saddle point equations change accordingly as $\hat{s}_k^t \rightarrow \hat{s}_k^t/\gamma$, $\hat{n}_k^t \rightarrow \hat{n}_k^t/\gamma$, $\hat{r} \rightarrow \hat{r}/\gamma$, while the order parameters $\{s_k^t, n_k^t\}$ remain unchanged; the stochastic action changes as $\Phi^* \rightarrow \Phi^*/\gamma$.

If we set the variance of arm k as $\sigma_k^2 = \gamma\tilde{\sigma}_k^2$, where $\tilde{\sigma}_k^2$ is a fixed parameter and γ can be varied (common to all arms), then the cumulative regret r follows a large deviation principle as

$$P(r|\sigma_k^2 = \gamma\tilde{\sigma}_k^2) \propto \exp\left(-\frac{1}{\gamma}I(r; \tilde{\sigma}_k^2)\right), \quad (38)$$

$$I(r|\tilde{\sigma}_k^2) \equiv \gamma\Phi^*(r|\sigma_k), \quad (39)$$

where $I(r|\tilde{\sigma}_k^2)$ is the rate function governing the rareness of regret r , and the order parameters $\{s_k^{*t}, n_k^{*t}\}$ at the saddle point dictates the most probable pathway leading to the regret r being specified¹⁸.

We remark that such a relation is derived in the limit $\sigma_k \rightarrow 0, \beta \rightarrow \infty$, but we expect some physical pictures can also be extended to cases with a finite noise strength. The approximation in Eq. (33) essentially neglects some fluctuation of the arm selection noise from the Boltzmann distribution in Eq. (9), which requires that the fluctuation due to a finite β in Eq. (9) is much smaller than the fluctuation from finite arm variances σ_k^2 (the limit of $\beta \rightarrow \infty$ is taken before the limit $\sigma_k \rightarrow 0$).

We also remark that the saddle point approach introduced above is only a leading-order approximation, and it is possible to derive higher-order corrections for a better accuracy¹⁶.

IV. RESULTS

In this section, we report the theoretical results from the above statistical-physics analysis on MABs in different scenarios, and corroborate them by numerical experiments.

We consider a bandit machine with $K = 3$ independent arms, where the reward of each arm k follows a Gaussian distribution $x_k \sim \mathcal{N}(\mu_k, \sigma_k^2)$. The arm distribution parameters are set to be $\boldsymbol{\mu} = [1, 2, 3]$, $\boldsymbol{\sigma} = \sqrt{\gamma}[1, 1, 1]$, which corresponds to setting $\tilde{\sigma}_k = 1$ in Eq. (38). One technical difficulty is to solve the highly nonlinear saddle point equations with $4K(T+1) + 1$ variables. Hence, we focus on systems with a relatively small number of time steps ($T \sim O(10)$), which already exhibits many interesting dynamical phenomena.

A. The Action Potential

To solve the saddle-point equations, we adopt an iteration method described in Appendix B in details. We found that in some parameter regime, the saddle point equations admit multiple solutions, in which cases we retained the solution with the smallest action potential Φ^* .

In Fig. 1, we sketch the resulting rescaled action potential $\gamma\Phi^*(r|\sigma^k)$ for different arm variance magnitude γ and different exploration parameter c , by fixing $\beta = 10$ and considering $T = 20$. The rescaled potential $\gamma\Phi^*(r|\sigma^k)$ predicted by the theory (black lines) exhibits a peculiar non-convex structure, comprised of 3 convex pieces (in general there are K convex pieces for K -armed bandits). This indicates a multimodal structure of the regret distribution $P(r)$ ⁹.

We also compare the theoretical prediction of the action potential to numerical simulations, obtained by simulating the corresponding MAB for 1×10^9 trials. The action potential for MABs by simulation is defined as

$$\Phi^{\text{sim}}(r) = -\log \hat{P}(r) - \min_r [-\log \hat{P}(r)], \quad (40)$$

where $\hat{P}(r)$ is the empirical density of the cumulative regret, and we have also subtracted $-\log \hat{P}(r)$ by its minimum. Under this definition, the minimal $\Phi^{\text{sim}}(r)$ is zero, which facilitates an easier comparison to the theory. We note that $\Phi^{\text{sim}}(r)$ loses the information about the precise value of $\hat{P}(r)$, but still carries the information of the relative strength between the probability densities of different regrets.

The results shown in Fig. 1 demonstrate a good match between theory and simulation for small and moderate arm variance level $\sqrt{\gamma}$. The difference between the two approaches becomes more prominent for large $\sqrt{\gamma}$, which is expected since the theory is developed in the small noise limit; but even in these cases, the qualitative trend of $\Phi^{\text{sim}}(r)$ still follows the theoretical prediction. In both theory and simulations, the action potential is asymmetric and right-skewed, which indicates that the MAB has a higher chance to be unlucky (the regret r is larger than the most probable value r^{mpv}) than lucky (the regret r is smaller than r^{mpv}). This is because being lucky mainly originates from the rarely good outcomes of many rounds from the optimal arm, but being unlucky originates from the rarely bad outcomes of a small number of rounds from

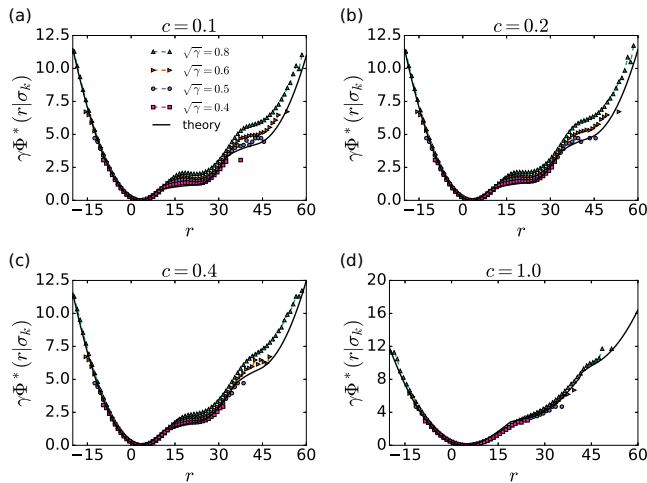


Figure 1. Rescaled action potential $\gamma\Phi^*(r|\sigma_k)$ as a function of the cumulative regret r . The black lines represent the theoretical predictions, while the dash lines with dots are obtained by numerical simulations of 1×10^9 trials. The parameters are $K = 3, T = 20, \beta = 10$. The theory in Sec. III B and III C predicts a universal rescaled action potential $\gamma\Phi^*(r|\sigma_k) = I(r|\tilde{\sigma}_k)$ in the low noise limit.

the optimal arm at the beginning, which makes it not well explored. The former occurs with a very small probability, while the latter occurs with a relatively higher probability. The heavy right tail of the regret distribution indicates a noticeable probability of the total arm rewards being sub-optimal in some realizations in a shot time, despite that the algorithm is optimal in the long run in the average sense^{9,14}.

B. Effect of the Exploration Parameter c

The noticeable probability for the system to have a high regret indicates that the system can be trapped into a state of excessive selections of sub-optimal arms (as will be shown in details below), which is partly due to insufficient exploration. This effect can be alleviated by increasing the exploration parameter c , as shown in Fig. 2(a). It is observed that for a higher c , the rate function $I(r|\tilde{\sigma}_k)$ attains larger values in the unlucky regime (with large positive regrets), indicating a much lighter tail for $P(r)$ for $r \gg 0$ and hence a much lower probability for more unlucky events.

On the other hand, increasing the exploration parameter c will increase the expected value of the regret, as the chance to explore sub-optimal arms also gets higher. Since it is not straightforward to measure the expected regret in theory since it involves the knowledge of the complete form of the rate function $I(r|\tilde{\sigma}_k)$ over the whole domain of r , we compute the most probable value of the regret r^{mpv} for different c , as shown in Fig. 2(b). It is observed that r^{mpv} increases very gently at the beginning, and starts to rise more significantly after $c \approx 0.4$. There-

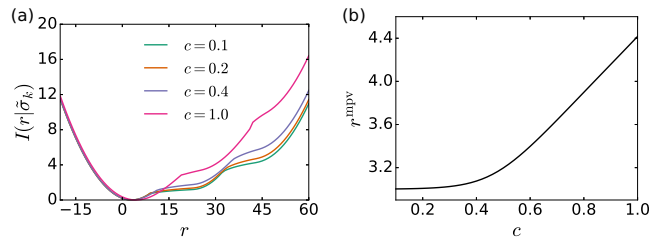


Figure 2. (a) The rate function $I(r|\tilde{\sigma}_k)$ predicted by the theory in the low noise limit $\beta \rightarrow \infty, \gamma \rightarrow 0$ as a function of regret r for different exploration parameters c . (b) The most probable value of regret $r^{\text{mpv}} = \arg \min_r I(r|\tilde{\sigma}_k)$ as a function of the exploration parameter c .

fore, the suppression of the right tail of the regret distribution $P(r)$ comes with a price of increasing the most probable regret. A risk-averse MAB algorithm needs to take these effects into account.

C. Dominant Trajectories

Another nice feature of the large deviation path-integral approach is that it can give rise to the dominant trajectories leading to a particular regret r . When the noise is small, the trajectory leading to the smallest action Φ^* at a particular r dominates the probability density $P(r)$ in the path integral Eq. (18). These dominant trajectories are also called the optimal paths or the instantons¹⁸. Here, we use the characteristics of the optimal paths derived from the small noise limit to explain the dynamics behaviors of MABs with a finite noise strength, which is of more practical interest. We also consider a small time window $T = 20$, which already provides many valuable insights.

1. Lucky and slightly unlucky events: Conditioned on $r = -8$ and $r = 6$

In Fig. 3, we consider the trajectories conditioned on a negative regret $r = -8$ and a small positive regret $r = 6$, which is considered as a lucky case and a slightly unlucky case. It is observed that in both cases, the optimal arm $k^* = 3$ is mostly chosen by the player after $t = 0$, and the trajectory leading to a particular regret r is due to homogeneous deviation of the realized reward $x_{k^*}^t$ at time t from the its expected value μ_* (as demonstrated in Fig. 3(a) and (c)). That is, the deviation $x_{k^*}^t - \mu_*$ is almost the same for all $t > 0$, which is akin to the “fluid phase” of independent random variables $\{x_i\}$ conditioned by the value of their sum²¹.

The theoretical prediction and numerical simulations match very well, although the arm noise is not small.

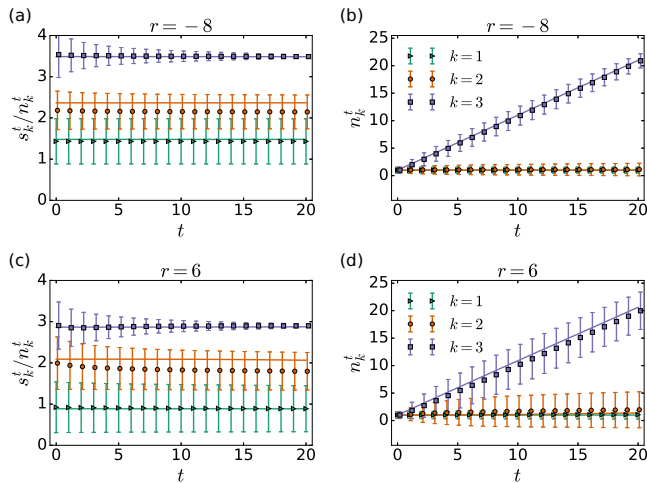


Figure 3. Dominant trajectories at a negative regret $r = -8$ (panel (a) and (b)) and a small positive regret $r = 6$ (panel (c) and (d)), revealed by the dynamical evolution of s_k^t/n_k^t and n_k^t . The lines represent the trajectories predicted by the theory. The dots with error bars are results from numerical simulations by simulating 1×10^9 trials and keeping the trajectories with cumulative regret $r^{\text{sim}} \in [r, r + 0.5)$; the error bars represent one standard deviation of the quantity measured in these trajectories. The parameters are $K = 3, T = 20, \beta = 10, c = 0.4, \sqrt{\gamma} = 0.6$.

2. Unlucky events: Conditioned on $r = 16$ and $r = 24$

In Fig. 4, we consider the unlucky cases with moderate regrets with $r = 16$ and $r = 24$, which enters the second convex branch of the potential $\Phi^*(r)$ shown in Fig. 1(c). Interestingly, the typical trajectory leading to $r = 16$ behaves as follows: the reward from the 3rd arm (the optimal arm) in the initial exploration stage is unluckily a bit lower than that from the 2nd arm (the sub-optimal arm), resulting in a substantial exploitation of the 2nd arm in the subsequent steps. During this process, n_2^t grows while n_3^t remains unchanged. Up to a certain point, the exploration term $c\sqrt{\log(K+t)/n_3^t}$ on the 3rd arm becomes large enough for the UCB index B_3^t of the 3rd arm to dominate that of the 2nd arm. After then, the player starts to collect rewards from the 3rd arm and gradually realize that it has a higher expected reward than the more exploited 2nd arm.

Similarly, for $r = 24$, the reward from the 3rd arm in the initial exploration step is also unluckily small, and it is even smaller than the case of $r = 16$. Therefore, the 2nd arm is being pulled throughout the process. As the gap between the empirical means $\frac{s_2^t}{n_2^t} - \frac{s_3^t}{n_3^t}$ is large in this case, the exploration term in the 3rd arm is not strong enough to overturn the exploitation of the 2nd arm in such a small time window, which is different from the case of $r = 16$.

Similar findings of the typical behaviors of the optimal arm leading to large regrets have also been reported be-

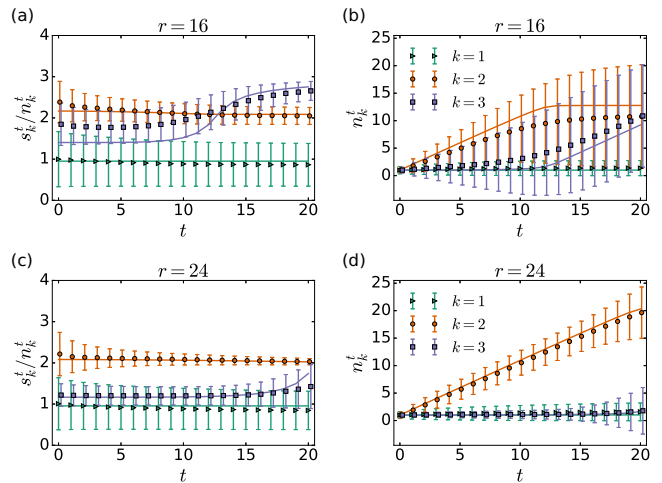


Figure 4. Dominant trajectories at regrets $r = 16$ (panel (a) and (b)) and $r = 24$ (panel (c) and (d)). The parameter setting is the same as those in Fig. 3.

fore^{9,14}. Our analytical method complements these studies and provides a much more detailed picture of the dominant trajectories in this regime.

3. Extremely unlucky events: Conditioned on $r = 36$ and $r = 40$

In Fig. 5, we consider the extremely unlucky cases with large regrets with $r = 36$ and $r = 40$, which enters the third convex branch of the potential $\Phi^*(r)$ shown in Fig. 1(c). The resulting phenomena are very similar to the cases in Sec. IV C 2, except that both the 3rd arm and the 2nd arm unluckily yield rewards smaller than the 1st arm (the worst arm). So the excess exploitation of the worst arm leads to such high regrets being considered.

Lastly, we notice that for trajectories conditioned on $r = 16$ and $r = 36$, numerical simulations exhibit very large fluctuations. In these cases, there exist many trajectories having similar values of Φ^* as the optimal path (e.g., there can be multiple solutions of the saddle point equations with similar potentials). Our theory just picks the one with the smallest Φ^* , the most probable trajectory, assuming a vanishing arm noise. However, when the noise is finite, different dominant and sub-dominant trajectories can coexist.

D. Exact Results of a Small System

In this section, we further investigate the nature of multiple solutions of the saddle point solution equations, which is related to the behavior of multiple branches of the action potential $\Phi^*(r|\sigma_k)$. To this end, we consider a small MAB system with $K = 2, T = 1$, and set the arm related parameters as $\mu = [1, 2], \sigma = \sqrt{\gamma}[1, 1]$. For such

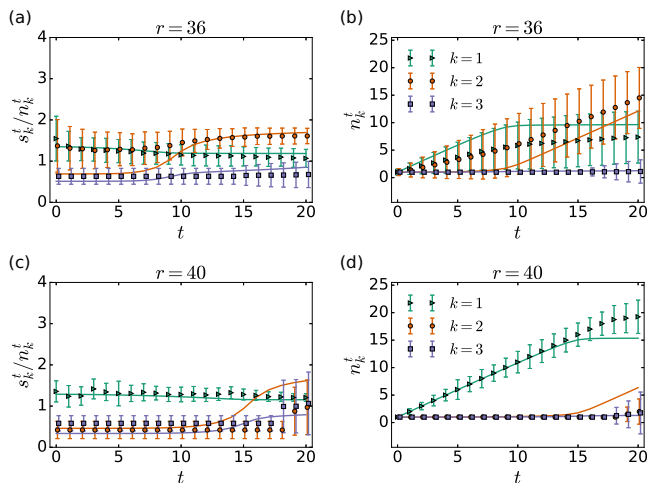


Figure 5. Dominant trajectories at regrets $r = 36$ (panel (a) and (b)) and $r = 40$ (panel (c) and (d)). The parameter setting is the same as those in Fig. 3.

a small system, the saddle point equations developed in Sec. III B and Sec. III C can be straightforwardly reduced to the following self-consistent equation of a single variable $\Delta s^0 = s_2^0 - s_1^0$,

$$g(\Delta s^0) = -2(\mu_2 - \mu_1)\beta\gamma\mathcal{S}(\beta\Delta s^0)[1 - \mathcal{S}(\beta\Delta s^0)]i\hat{r}(\Delta s^0) + (\mu_2 - \mu_1) - \Delta s^0 = 0, \quad (41)$$

$$i\hat{r}(\Delta s^0) = \frac{(\mu_2 - \mu_1)[\mathcal{S}(\beta\Delta s^0) - 2] + r}{3\gamma}, \quad (42)$$

where we have defined the sigmoid function $\mathcal{S}(x) := 1/(1 + e^{-x})$.

The root Δs^{0*} of the equation $g(\Delta s^0) = 0$ (for a given r) is a stationary point of Φ . We set $\sqrt{\gamma} = 0.4, \beta = 10$ and identify all possible solutions for different regrets; the results are shown in Fig. 6. For $r < r_c \approx 1.9533$, there is only one branch of solution with $\Delta s^{0*} \approx 1 (= \mu_2 - \mu_1)$; this corresponds to the “liquid phase” where the arm rewards deviate from their expected value homogeneously. For $r > r_c \approx 1.9533$, the system develops two additional branches of stationary solutions, where the optimal arm unluckily yields a small reward. The three branches of stationary solutions for large regrets correspond to two local minima (the 1st and 2nd branches in Fig. 6) separated by a saddle point (the 3rd branch in Fig. 6) in the action potential in the space of order parameters. In the small noise limit, the branch with the smallest potential Φ^* dominates the probability density. In the case with a finite noise strength, trajectories of different branches can coexist.

V. CONCLUSION

In summary, we employed the path-integral method from statistical physics to examine the complex dynam-

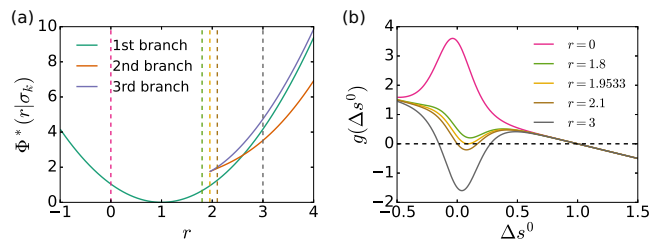


Figure 6. Behaviors of a small MAB with $K = 2, T = 1$. We set the parameters as $\sqrt{\gamma} = 0.4, \beta = 10$. (a) The stationary action potential $\Phi^*(r|\sigma_k)$ determined by Eq. (41). (b) The left-hand side of the self-consistent equation $g(\Delta s^0)$ defined in Eq. (41).

ics of multi-armed bandits, which are classical prototypical models for understanding decision-making and optimization in uncertain environments and the dilemma between exploration and exploitation. By mapping the MABs under the UCB algorithm onto stochastic dynamical systems and considering the low temperature and small noise limit, we derived a large deviation formalism for the cumulative regrets of MABs, from which many valuable insights of the regret distribution and the dominant trajectory leading to a certain regret were obtained, revealing the transient dynamics leading lucky, unlucky or even extreme events.

We observed that the action potential of the MABs can be non-convex, indicating the multimodal structure of the regret distribution. We showed that such a multimodal structure is due to the existence of multiple solutions of the saddle point equations when the regret is larger than a threshold. Under the UCB algorithm, the MABs have a much higher chance to be unlucky (the regret is higher than expected) than lucky (the regret is lower than expected), where the chance of being unlucky depends on the strength of exploration. The dominant trajectories leading to high regrets are those where the optimal arm unluckily yields a small reward in the initial exploration stage, such that it is much less exploited in the subsequent time steps.

Despite a relatively small time window being considered, our study uncovered many interesting characteristics of the MABs as complex systems. Extending the analysis to larger systems and longer time windows requires a sophisticated method to solve the high-dimensional nonlinear saddle point equations, which contributes the construction of new methodology as well as a new understandings on MABs, exploitation-exploration dilemma, as well as the origin and occurrence of extremely unlucky events. We envisage that the methods developed in this work can provide a valuable tool for analyzing different variants of MABs and other complex stochastic decision-making processes.

ACKNOWLEDGMENTS

We thank David Saad for helpful discussions. B.L. acknowledges support from the Leverhulme Trust (RPG-2018-092), European Union's Horizon 2020 research and innovation programme under the Marie Skłodowska-Curie Grant Agreement No. 835913 and the startup funding from Harbin Institute of Technology, Shenzhen (Grant No. 20210134). C.H.Y. is supported by the Research Grants Council of the Hong Kong Special Administrative Region, China (Projects No. EdUHK GRF 18304316, No. GRF 18301217, and No. GRF 18301119), the Dean's Research Fund of the Faculty of Liberal Arts and Social Sciences (Projects No. FLASS/DRF 04418, No. FLASS/ROP 04396, and No. FLASS/DRF 04624), and the Internal Research Grant (Project No. RG67 2018-2019R R4015 and No. RG31 2020-2021R R4152), The Education University of Hong Kong, Hong Kong Special Administrative Region, China.

AUTHOR DECLARATIONS

A. Conflict of Interest

The authors have no conflicts to disclose.

B. Author Contributions

Bo Li: Conceptualization (equal); Methodology (equal); Formal Analysis (lead); Software (lead); Writing – original draft (lead). **Chi Ho Yeung:** Conceptualization (equal); Methodology (equal); Formal Analysis (supporting); Software (supporting); Writing – original draft (supporting).

DATA AVAILABILITY STATEMENT

Data sharing is not applicable to this article as no new data were created or analyzed in this study.

Appendix A: Details of the Path-integral Formalism

In this section, we supplement some details of the path integral calculation.

To perform integration over the disorder variables $x_k^{1:T}$,

we first notice

$$\begin{aligned} \sum_{t=1}^T \hat{s}_k^t \left[\sum_{\tau=1}^t x_k^\tau \delta(a^\tau, k) \right] &= \sum_{t=1}^T \hat{s}_k^t \left[\sum_{\tau=1}^T x_k^\tau \delta(a^\tau, k) \mathbb{I}(t \geq \tau) \right] \\ &= \sum_{\tau=1}^T x_k^\tau \delta(a^\tau, k) \left[\sum_{t=1}^T \hat{s}_k^t \mathbb{I}(t \geq \tau) \right] \\ &= \sum_{\tau=1}^T x_k^\tau \delta(a^\tau, k) \left[\sum_{t=\tau}^T \hat{s}_k^t \right] = \sum_{t=1}^T x_k^t \delta(a^t, k) \left[\sum_{\tau=t}^T \hat{s}_k^\tau \right], \end{aligned} \quad (\text{A1})$$

where we have switched the dummy time indices t and τ in the last line.

Then for the terms relevant to $x_k^{1:T}$, we have

$$\begin{aligned} &\int \prod_{t=1}^T dx_k^t \mathcal{N}(x_k^t | \mu_k, \sigma_k^2) \exp \left\{ i \sum_{t=1}^T x_k^t \delta(a^t, k) \left[\sum_{\tau=t}^T \hat{s}_k^\tau \right] \right\} \\ &= \exp \left\{ -\frac{1}{2} \sigma_k^2 \sum_{t=1}^T \delta(a^t, k) \left[\sum_{\tau, \tau'=t}^T \hat{s}_k^\tau \hat{s}_k^{\tau'} \right] \right. \\ &\quad \left. + i \mu_k \sum_{t=1}^T \delta(a^t, k) \left[\sum_{\tau=t}^T \hat{s}_k^\tau \right] \right\}, \end{aligned} \quad (\text{A2})$$

where we have made use of the characteristic function of Gaussian distribution $\int e^{-ixh} \mathcal{N}(x | \mu, \sigma^2) dx = e^{-\frac{1}{2} \sigma^2 h^2 - i\mu h}$ and the idempotence property of Kronecker delta $\delta(a^t, k)^2 = \delta(a^t, k)$.

The first term in the exponent of Eq. (A2) can be rearranged as

$$\begin{aligned} &\sum_{t=1}^T \delta(a^t, k) \left[\sum_{\tau, \tau'=t}^T \hat{s}_k^\tau \hat{s}_k^{\tau'} \right] \\ &= \sum_{t=1}^T \delta(a^t, k) \left[\sum_{\tau, \tau'=1}^T \hat{s}_k^\tau \hat{s}_k^{\tau'} \mathbb{I}(\tau \geq t) \mathbb{I}(\tau' \geq t) \right] \\ &= \sum_{\tau, \tau'=1}^T \hat{s}_k^\tau \hat{s}_k^{\tau'} \left[\sum_{t=1}^{\min(\tau, \tau')} \delta(a^t, k) \right] \\ &= \sum_{\tau, \tau'=1}^T \hat{s}_k^\tau \hat{s}_k^{\tau'} (n_k^{\min(\tau, \tau')} - 1), \end{aligned} \quad (\text{A3})$$

where we have made use of the definition of n_k^t .

Similarly, we have

$$\begin{aligned} \sum_{t=1}^T \delta(a^t, k) \left[\sum_{\tau=t}^T \hat{s}_k^\tau \right] &= \sum_{\tau=1}^T \hat{s}_k^\tau \left[\sum_{t=1}^{\tau} \delta(a^t, k) \right] \\ &= \sum_{\tau=1}^T \hat{s}_k^\tau (n_k^\tau - 1). \end{aligned} \quad (\text{A4})$$

Integration over x_k^0 for the relevant terms gives

$$\begin{aligned} & \int dx_k^0 P(x_k^0) \exp \left\{ ix_k^0 \left[\sum_{\tau=1}^T \hat{s}_k^\tau \right] \right\} \\ &= \exp \left\{ -\frac{1}{2} \sigma_k^2 \left[\sum_{\tau, \tau'=0}^T \hat{s}_k^\tau \hat{s}_k^{\tau'} \right] + i\mu_k \left[\sum_{\tau=0}^T \hat{s}_k^\tau \right] \right\}. \quad (\text{A5}) \end{aligned}$$

Collecting the above results gives rise to the stochastic action defined in Eq. (18) and Eq. (19).

Appendix B: Iteration Method for Solving the Saddle-point Equations

Grouping all order parameters as a big vector $\mathbf{y} := [\mathbf{s}^{0:T}, \mathbf{n}^{0:T}, i\hat{\mathbf{s}}^{0:T}, i\hat{\mathbf{n}}^{0:T}]$, the saddle point equations have the form of

$$\mathbf{y} = f(\mathbf{y}; i\hat{r}), \quad (\text{B1})$$

$$\sum_k s_k^T = (T+k)\mu_* - r, \quad (\text{B2})$$

where the nonlinear mapping $f(\cdot)$ is the right-hand side of the saddle point equations involving \mathbf{y} given in Sec. III B and Sec. III C.

Given a random initial guess of the solution $[\mathbf{y}, i\hat{r}]$, the iteration method iteratively performs the following two steps until convergence

1. $\mathbf{y}^{\text{new}} = \alpha f(\mathbf{y}^{\text{old}}, i\hat{r}^{\text{old}}) + (1-\alpha)\mathbf{y}^{\text{old}}$,
2. update $i\hat{r}$ to bring $\sum_k s_k^T$ closer to $(T+k)\mu_* - r$.

The second step is difficult to achieve as s_k^T depends intricately on $i\hat{r}$. In this step, we adopt a heuristic treatment of Eq. (27) (for the final time $t = T$) as

$$s_k^T(i\hat{r}) = \sigma_k^2 (i\hat{s}_k^T) n_k^T + \mu_k n_k^T + \sigma_k^2 \sum_{t'=0}^{T-1} (i\hat{s}_k^{t'}) n_k^{t'}, \quad (\text{B3})$$

$$= -(i\hat{r}) \sigma_k^2 n_k^T + \text{const w.r.t. } i\hat{r}, \quad (\text{B4})$$

which we only retain the dependence of $i\hat{s}_k^T$ on $i\hat{r}$ (remind that $i\hat{s}_k^T = -i\hat{r}$) and consider the dependence of n_k^t and $i\hat{s}_k^{t'}$ for $t' < T$ on $i\hat{r}$ as a weaker effect.

The above iteration method does not converge in some problem instances of MABs, in which cases it still leads to significant reduction of the residual

$$\text{res} = \|\mathbf{y} - f(\mathbf{y}; i\hat{r})\|^2 + \left(\sum_k s_k^T + r - (T+k)\mu_* \right)^2. \quad (\text{B5})$$

In these cases, we use the final outcome of the iteration method as an initial guess of the solution, which is fed to a nonlinear solver (e.g., by Newton's method) to find the root of the saddle point equation.

REFERENCES

- ¹Gandhimohan. M. Viswanathan, Marcos G. E. da Luz, Ernesto P. Raposo, and H. Eugene Stanley. *The Physics of Foraging: An Introduction to Random Searches and Biological Encounters*. Cambridge University Press, 2011.
- ²Sofia S. Villar, Jack Bowden, and James Wason. Multi-armed Bandit Models for the Optimal Design of Clinical Trials: Benefits and Challenges. *Statistical Science*, 30(2):199 – 215, 2015.
- ³Hagit Grushka-Cohen, Raphael Cohen, Bracha Shapira, Jacob Moran-Gilad, and Lior Rokach. A framework for optimizing covid-19 testing policy using a multi armed bandit approach. *arXiv:2007.14805*, 2020.
- ⁴Richard S. Sutton and Andrew G. Barto. *Reinforcement Learning: An Introduction*. A Bradford Book, MIT press, Cambridge, MA, USA, 2018.
- ⁵Sébastien Bubeck and Nicolò Cesa-Bianchi. Regret analysis of stochastic and nonstochastic multi-armed bandit problems. *Foundations and Trends® in Machine Learning*, 5(1):1–122, 2012.
- ⁶Aleksandrs Slivkins. Introduction to multi-armed bandits. *Foundations and Trends® in Machine Learning*, 12(1-2):1–286, 2019.
- ⁷T.L Lai and Herbert Robbins. Asymptotically efficient adaptive allocation rules. *Advances in Applied Mathematics*, 6(1):4–22, 1985.
- ⁸Bobak Shahriari, Kevin Swersky, Ziyu Wang, Ryan P. Adams, and Nando de Freitas. Taking the human out of the loop: A review of bayesian optimization. *Proceedings of the IEEE*, 104(1):148–175, 2016.
- ⁹Jean-Yves Audibert, Rémi Munos, and Csaba Szepesvári. Exploration–exploitation tradeoff using variance estimates in multi-armed bandits. *Theoretical Computer Science*, 410(19):1876–1902, 2009. Algorithmic Learning Theory.
- ¹⁰Antoine Salomon and Jean-Yves Audibert. Deviations of stochastic bandit regret. In Jyrki Kivinen, Csaba Szepesvári, Esko Ukkonen, and Thomas Zeugmann, editors, *Algorithmic Learning Theory*, pages 159–173, Berlin, Heidelberg, 2011. Springer Berlin Heidelberg.
- ¹¹Amir Sani, Alessandro Lazaric, and Rémi Munos. Risk-aversion in multi-armed bandits. In F. Pereira, C.J. Burges, L. Bottou, and K.Q. Weinberger, editors, *Advances in Neural Information Processing Systems*, volume 25, pages 3275–3283. Curran Associates, Inc., 2012.
- ¹²Nicolas Galichet, Michèle Sebag, and Olivier Teytaud. Exploration vs exploitation vs safety: Risk-aware multi-armed bandits. In Cheng Soon Ong and Tu Bao Ho, editors, *Proceedings of the 5th Asian Conference on Machine Learning*, volume 29 of *Proceedings of Machine Learning Research*, pages 245–260, Australian National University, Canberra, Australia, 2013. PMLR.
- ¹³Stefan Wager and Kuang Xu. Diffusion asymptotics for sequential experiments. *arXiv:2101.09855*, 2021.
- ¹⁴Lin Fan and Peter W. Glynn. Diffusion approximations for thompson sampling. *arXiv:2105.09232*, 2021.
- ¹⁵Hugo Touchette. The large deviation approach to statistical mechanics. *Physics Reports*, 478(1):1–69, 2009.
- ¹⁶John A Hertz, Yasser Roudi, and Peter Sollich. Path integral methods for the dynamics of stochastic and disordered systems. *Journal of Physics A: Mathematical and Theoretical*, 50(3):033001, 2016.
- ¹⁷Peter Auer, Nicolò Cesa-Bianchi, and Paul Fischer. Finite-time analysis of the multiarmed bandit problem. *Machine Learning*, 47:235–256, 2002.
- ¹⁸Tobias Grafke and Eric Vanden-Eijnden. Numerical computation of rare events via large deviation theory. *Chaos: An Interdisciplinary Journal of Nonlinear Science*, 29(6):063118, 2019.
- ¹⁹Pierre Paga and Reimer Kühn. Large deviations of the finite-time magnetization of the curie-weiss random-field ising model. *Phys. Rev. E*, 96:022126, Aug 2017.
- ²⁰Bo Li and David Saad. Large deviation analysis of function sensitivity in random deep neural networks. *Journal of Physics A:*

Mathematical and Theoretical, 53(10):104002, feb 2020.

²¹Claude Godrèche. Condensation for random variables condi-

tioned by the value of their sum. *Journal of Statistical Mechanics: Theory and Experiment*, 2019(6):063207, jun 2019.